Distribution Agreement

In presenting this thesis as a partial fulfillment of the requirements for a degree from Emory University, I hereby grant to Emory University and its agents the non-exclusive license to archive, make accessible, and display my thesis in whole or in part in all forms of media, now or hereafter now, including display on the World Wide Web. I understand that I may select some access restrictions as part of the online submission of this thesis. I retain all ownership rights to the copyright of the thesis. I also retain the right to use in future works (such as articles or books) all or part of this thesis.

Benjamin Kasavan April 9, 2019

A Study of the Physical Properties of Acrylic Polymers Commonly Used in Art Conservation

by

Benjamin L. Kasavan

Connie B. Roth
Adviser

Department of Physics

Connie B. Roth

Adviser

Justin C. Burton

Committee Member

Renée A. Stein

Committee Member

2019

A Study of the Physical Properties of Acrylic Polymers Commonly Used in Art Conservation

By

Benjamin L. Kasavan

Connie B. Roth

Adviser

An abstract of
a thesis submitted to the Faculty of Emory College of Arts and Sciences
of Emory University in partial fulfillment
of the requirements of the degree of
Bachelor of Sciences with Honors

Department of Physics

2019

Abstract

A Study of the Physical Properties of Acrylic Polymers Commonly Used in Art Conservation
By Benjamin L. Kasavan

Acrylic polymers, such as A-11, B-72, B-48N, and B-44, are regularly used in art conservation to adhere parts together, to consolidate friable objects, and to coat objects, protecting them from light and water. The effect of the glass transition has previously been found to have a large impact on the working properties of these polymers. Furthermore, recent work has sought to mix B-72 and B-48N together in the hope that the blend would provide better properties than either material on its own.

In this study, I used ellipsometry to study the pure polymers, characterizing how the thickness, refractive index, and thermal expansivity go through the glass transition. By comparing the information gleaned on the pure polymers to the data available in the literature, I was able to determine that B-72, B-44, and A-11 all have relatively small breadths in their glass transitions, with the main difference being the temperature at which they start. B-48N had an extremely broad transition spanning more than twice the temperature range of the other polymers. I also showed that mixing B-72 and B-48N in a 3:1 ratio gave a higher glass transition temperature T_g than pure B-72, with a narrower transition than B-48N. The 1:3 B-72:B-48N mixture of the two polymers gave a T_g that is 5 °C higher than the 3:1 mixture, at the expense of a slightly broader transition, suggesting that this combination may have better stability when the object is exposed to temperatures over 40 °C, as may occur when exposed to direct sunlight.

A Study of the Physical Properties of Acrylic Polymers Commonly Used in Art Conservation

By

Benjamin L. Kasavan

Connie B. Roth

Adviser

A thesis submitted to the Faculty of Emory College of Arts and Sciences
of Emory University in partial fulfillment
of the requirements of the degree of
Bachelor of Sciences with Honors

Department of Physics

2019

Acknowledgements

I will first and foremost say thank you to Juno, the cat I live with for the constant and consistent support she gave me throughout writing. While she may have waited a few hours for dinner at times because of this thesis, she was perfect. I would also like to thank all the members of the Roth research group. Specifically, I want to thank Olivia Boyd with whom I collaborated on this project and who will be continuing it once I leave this wonderful group. I also want to thank Michael Thees for his consistent answers to my one sentence questions emailed at 11pm, as well as Jennifer McGuire for being a critically helpful sounding board for my ideas.

I also want to thank Jessica Betz: not only does this work build off of hers, she was also invaluable in discussions about how we can interpret our data. I also sincerely thank Renee Stein and Justin Burton for serving on my committee, and providing helpful feedback, and, in the case of Ms. Stein, helping me understand the field of art conservation, to which I had previously been unexposed. Finally, I have a sincere thank you to my advisor Connie Roth for her immense help in leading my research and for being a phenomenal mentor.

Table of Contents

Table of Figures and Tables

Chapter 1: Introduction and Background

1.1: Art Conservation

Art conservation seeks to preserve artistic and historical objects by treating them in a way that prevents further deterioration and promotes their longevity, enabling them to be studied, stored, and displayed. This goal leads to three important guiding principles when choosing what materials will be used to conserve an object, which will be discussed in depth below: its stability, its reversibility, and not detracting from the original appearance.[1]

It is crucial that the restoration, conservation, and display methods of an object be as stable as the application calls for. Most applications will call for an adhesive that can last over a hundred years, for example when adhering two parts of a statue back together. This will prevent future damage to the object if the polymer were to fail.[2]

History has shown us it is very likely that the future will bring better, more stable, or less visible materials for conserving objects.[1] An example is cellulose nitrate, which was widely used in the early 20th century and which darkens over time, leading to visible discoloration where the object had been repaired or coated. B-72 is a preferable alternative to cellulose nitrate due to its stability and ease of use.[3]

To allow for future changes to an object, or new interpretations and opinions about the repair, all repairs and restorations made to an object should be, to the greatest extent possible, reversible.[4,5] The very act of restoring an object might be later deemed unacceptable, as the object with visible deterioration might be considered a more faithful version than the one with the restoration. Related to reversibility is also a desire that any future failure of the join will damage the polymer and not the original object. When adhering two pieces of an object together,

this means that the adhesive in the joint should be weaker than the parts that it is holding together.[6]

A final goal of a conservation treatment is to have the object appear as originally intended, or at least not significantly altered from its current state. This goal requires that the materials used should either be invisible, or should be able to blend in seamlessly with the object.

The stability and longevity of a treatment is affected by the conditions in which the object is stored or displayed. While many of the commonly used treatment materials work well in the controlled temperature, humidity, and lighting found inside museums, they may not work as well when used outdoors on archaeological sites or in contemporary artwork installations where the conditions are more extreme and variable.[2,7] The most important difference between indoor and outdoor settings for objects is the higher temperatures the object may be exposed to which can lead to significant changes in the adhesive's properties. In addition to this risk, significant changes in temperature can cause a degradation of the bond due to the thermally induced expansion and contraction, leading to the degradation of the adhesive and failure of the repair or coating.[5,6]

1.2: Polymer Properties

Polymers are long molecules that are composed of a long chain of repeating units called monomers. Polymers are commonly used in applications all around us from rubber tires to Styrofoam. At high temperatures the polymer segments have enough energy to move around and remain in an equilibrium configuration when the temperatures changes. When at temperatures where this is the case, the polymer exists in a rubbery state. As the temperature decreases, there will be a point where the polymer segments can no longer rearrange into a new equilibrium state

with the changing temperature leaving them “frozen” in a non-equilibrium glass. The temperature at which a polymer passes from a rubber to a glass is called the glass transition temperature T_g. In the rubbery and glassy regimes the density and refractive index of a polymer change linearly with temperature. The T_g can be fit by finding the intersection of these two lines, as shown Figure 1.1. The refractive index is a dimensionless number that describes how light propagates through a medium. Differences in refractive index between transparent objects lead to refraction and reflection at interfaces: this is what causes a pencil in a glass of water to appear to bend when it goes from air ($n \approx 1$) to water ($n \approx 1.3$).[1,8]

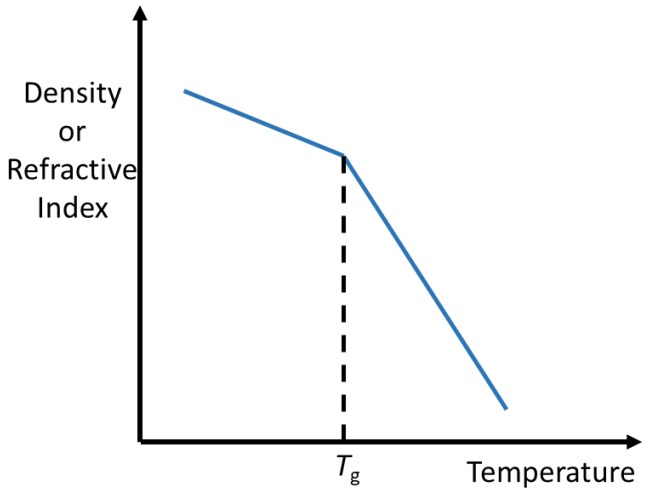

Figure 1.1: Illustration of how the density or refractive index of a polymer changes with temperature before and after the glass transition temperature T_g.

The thermal expansivity is a measure of how much a material expands or contracts when it is heated or cooled. Above and below T_g, the thermal expansivity of a polymer is relatively constant, however near T_g it changes very rapidly. As shown in Figure 1.2, the T_g can be defined as the midpoint between the onset and endpoint temperatures. This method should give a T_g that

is equivalent to measuring T_g with the intersection of the glassy and rubbery lines from density changes.[9]

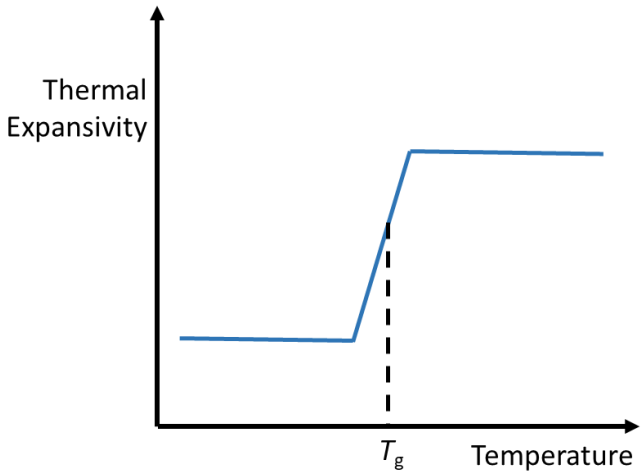

Figure 1.2: Illustration of how the thermal expansivity of a polymer changes with temperature before and after the glass transition temperature T_g. The T_g can be defined as the midpoint between the beginning and the end of the thermal expansivity change.

The measured T_g depends on polymer segments being unable to rearrange into equilibrium as the polymer cools, which means that the time scale on which an experiment occurs will affect what T_g is measured. If the volume of a polymer is measured with a fast cooling rate, as shown in Figure 1.3, T_{g1} can be found. If the sample is then measured with a slower cooling rate, a lower T_{g2} can be found. A glass which is formed quickly will have a larger volume and a structure that is further from equilibrium, leading it to being less stable over time. This is an important fact to keep in mind in art conservation where an item conserved with a polymer will apply stresses to it for a period of years. In *Materials for Conservation*, Horie[1] illustrates this point by stating that "a material with T_g of 30 °C (measured over 1 minute) will

have an effective T_g of 12 °C when used on an object for 1.2 years." This decreased T_g can be seen when fragments of an objects which were joined together slump over time.[1]

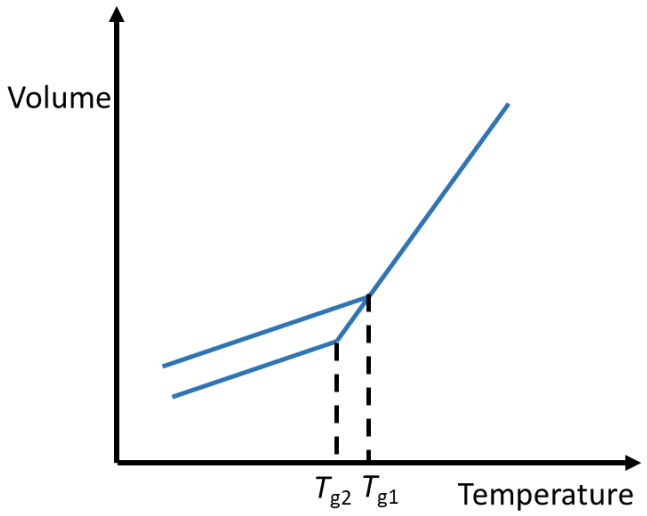

Figure 1.3: Illustration of how the volume of a polymer changes with temperature before and after the glass transition temperature T_g when cooled with two separate cooling rates. T_{g1} happens with a fast cooling rate, while T_{g2} happens with a slow cooling rate.

In a pure material, the T_g of a polymer is a property mainly related to its chemical structure. This relationship is summarized in Table 1.1. In conservation, however, polymers are often used by dissolving them in a solvent and then letting the solvent evaporate. The presence of solvent molecules effectively decreases the T_g of the polymer. As the solvent evaporates in a polymer with a T_g above ambient temperature, the T_g of the material will increase until it is higher than the ambient temperature at which point there will still be trapped solvent molecules that will evaporate very slowly.[1,10]

Name	Chemical Formula	T_g (°C)[10]
Methyl Methacrylate	$C_5H_8O_2$	105
Ethyl Methacrylate	$C_6H_{10}O_2$	65
Butyl Methacrylate	$C_8H_{14}O_2$	20
Methyl Acrylate	$C_4H_6O_2$	9
Ethyl Acrylate	$C_5H_8O_2$	-22

Table 1.1: Chemical formula of monomers used in this study and T_g of the polymers created from those monomers.

Polymer properties can also be modified with plasticizers. Plasticizers are small molecules which when added to a polymer change its properties, generally leading to a lower T_g, and greater flexibility. Solvent remaining in a polymer effectively acts as a plasticizer, reducing the T_g of the polymer while it is present.[1]

1.3: Acrylic Polymers Used in Art Conservation

There are three main uses for acrylic adhesives in art conservation: as an adhesive, as a consolidant, and as a coating. Polymers are used as an adhesive when joining separate pieces back together. Consolidants are used by placing a dilute solution of the polymer on the outside of an object to strengthen it and prevent dust or paint flakes from falling off. Coatings seek to inhibit interactions between the object and the environment, for example isolating it from oxygen and water to slow down rusting.[1,10] In our study we will be looking at four polymers used in art conservation produced by Rohm and Haas. They are commonly known by their commercial

names Paraloid A-11, B-72, B-48, and B-44, and their properties are summarized in Table 1.2. Their weight average molecular weights are between 100 000 and 250 000 g/mol.[10]

Name	Monomer content[10]	Solvents commonly used[1,10]	Reported T_g[1,10]	Refractive Index
A-11	100% methyl methacrylate	Methyl ethyl ketone (MEK), toluene, ethyl acetate.[11]	100 °C	1.49 [12]
B-72	32% methyl acrylate, 65.8% ethyl methacrylate, 2.2% butyl methacrylate	Acetone, toluene, xylene, p-xylene.[1,13]	40 °C	1.48 [1]
B-48N	74.5% methyl methacrylate, 25.5% butyl methacrylate	Toluene + ethanol, xylene, MEK, acetone.[14]	50 °C	1.48 [1]
B-44	28% ethyl acrylate, 70% methyl methacrylate	Acetone, toluene, xylene, MEK.[15]	60 °C	1.48 [1]

Table 1.2: Summary of the properties of the polymers used in this study.

The four studies described by Horie[1] which report the refractive index of B-72 give a value of refractive index of 1.481 ± 0.005. All the index values reported for the other polymers fall within this error, and within two significant figures are equal to 1.48. This gives an average index 1.480 ± 0.003 for all of the polymers in this study, where the error is equal to the standard deviation between the different values of index. Indices are reported at $\lambda = 598$ nm (sodium D line) to match what is generally reported in the literature.

A-11 is commonly used for coating metal, vinyl, and plastic. It consists of a pure methyl methacrylate backbone, and has a reported T_g of 100 °C. It is generally considered to be one of the hardest acrylic polymers used in conservation, and is often avoided due to its brittleness.[1,10] It is pure poly(methyl methacrylate) (PMMA), also known as Plexiglas. PMMA is a polymer we have a lot of experience with in our research group; we studied A-11 as a control to ensure that our measurements matched what we would expect.

B-72 is one of the most common acrylic polymers used in art conservation, and is regarded as one suitable in almost every application, whether it be as a coating, a consolidant, or an adhesive.[3] Its monomers consist of methyl acrylate and ethyl methacrylate. Chiantore and Lazzari[16] independently studied the composition of B-72 by thermally degrading the polymer into its monomer constituents and analyzing those using gas chromatography. They found that there was approximately 2% butyl methacrylate in B-72 that was not reported by the manufacturer.[16] The reported T_g of B-72 is 40 °C.[1,10]

The use of B-72 has increased greatly since Koob[3] published a paper in 1986 advocating for its use as a structural adhesive.[1] In this paper, he also gave specific instructions on how it should be used, which are well known within art conservation. It involves dissolving B-72 in acetone at a 1:1 weight to weight ratio, with the B-72 suspended in a cotton bag to help it dissolve. This solution is placed in an aluminum tube to facilitate application and squeezed onto the prepared fragments of the object in a thin uniform line. The fragments are then connected and separated again to ensure that the adhesive has covered the entire joint and to allow some more solvent to evaporate. After holding them apart for a few seconds, the fragments must be held together for 10-20 seconds, at which point the joint will usually hold its own weight while the rest of the solvent evaporates. He also recommends sometimes adding fumed silica in order to improve the properties of the polymer.[3]

B-48N is often used as a coating for metals, and is known for its durability and its environmental stability.[10] It is a copolymer of methyl methacrylate and butyl methacrylate with a reported T_g of 50 °C.[1,10]

Our last polymer is B-44, a copolymer of ethyl acrylate and methyl methacrylate, which is usually used as a protective coating for metals in order to prevent corrosion and other effects

when outdoors.[10] It has also been reported to become insoluble after a period of 10 years, likely due to crosslinking.[1,10]

Finally, we are also investigating mixtures of B-72 and B-48N, which were used in the well documented reconstruction of Tullio's *Adam* after it broke while on display at the Metropolitan Museum of Art.[6] The team reconstructing the statue used a 3:1 mixture, where B-72 constituted the majority of the adhesive. In order to investigate the importance of the ratio in which the two polymers were mixed, Jessica Betz[10] investigated the mechanical properties of a 3:1 mixture of B-72 and B-48N, as well as a 1:3 mixture of them. She found that both mixtures performed very similarly and that even in small amounts the B-48N seems to control the performance of the system.

Koob's suggested method of using B-72, which is sometimes used for other acrylic polymers, leads to a rapid solvent evaporation which will create a glass that is similar to that created by a high cooling rate: one that will have a larger volume and thus be more brittle than one which was created by a slower evaporation or cooling rate. The faster solvent evaporation rate will lead to a glass which is further from equilibrium and less stable. This is offset by the non-constant evaporation rate: while the acetone will evaporate quickly when the joint is reopened, it is reconnected, lowering the evaporation rate. This low evaporation rate which occurs while the B-72 is above its glass transition leaves a glass which is closer to equilibrium than if the high evaporation rate had continued throughout the glass formation process. In the case of some of our polymers with a low T_g, notably B-72, because its T_g is close to room temperature, the polymer will be able to relax within the joint for a long period of time during solvent evaporation. A complicating factor is related to different evaporation rates of the solvent in different materials (depending on their porosity, and the size of the bond), as well as in

different uses: when used on a surface, as a coating or a consolidant, the solvent will evaporate much more quickly than it will when inside a joint, when the polymer is used as an adhesive.

Choices about materials are often guided by experience of which materials performed well in the past. Information about these materials come from three main sources. The first is from past experience by the conservator, and others in the field of art conservation in using it, as well as what was reported about their use in conference proceedings and publications. The second is the information provided by the manufacturer, which is generally related to the needs of its major users which are not conservators. Finally there are a few scientific studies of specific properties of the polymers which are often too specific to easily compare to the behavior of the materials when used on objects.[1] There are scientific studies characterizing the mechanical properties of these polymers,[10] as well as studies which investigate the chemical stability of the polymers.[7,16] We are seeking to study the glass transition of the polymers, including the breadth of the transitions, and to correlate this to the properties observed by conservators.

1.4: Goal and Outline of Thesis

The goal of this thesis is to study the physical properties of acrylic polymers commonly used in art conservation, and correlate these to the properties observed by conservators using them to conserve objects in museums. This will allow conservators to better predict how polymers will react in less controlled conditions as well as making it easier to compare the different polymers. The polymers will be studied with ellipsometry to determine their refractive index, thermal expansivity, and normalized film thickness as a function of temperature from which their T_g will be extracted.

Chapter 2: Optics and Ellipsometry

Light consists of an electromagnetic wave created by the superposition of many electric fields pointing in all directions perpendicular to the direction of travel. Each of these electric fields can be described by separate wave equations with different arbitrary phases and amplitudes. In a system such as ours where polarized light is reflecting off a surface, the electric field polarized in the plane of incidence (E_p) is called *p* polarized, while the one with a polarization normal to the plane of incidence (E_s) is called *s* polarized, as shown in Figure 2.1. In this case the light is created by the superposition of E_p and E_s which can be described with the following equations where E_0 refers to the amplitude of the field, λ refers to its wavelength, v is the speed of the wave, and ξ is an arbitrary phase, and the subscripts refer to which electric field we are talking about:[17]

$$E_p(z,t) = E_{0,p}\sin\left(\frac{2\pi}{\lambda}(z-vt)+\xi_p\right)$$

$$E_s(z,t) = E_{0,s}\sin\left(\frac{2\pi}{\lambda}(z-vt)+\xi_s\right).$$

The light is linearly polarized if the phase shifts ξ_p and ξ_s are equal to each other, or if $E_{0,p}$ or $E_{0,s}$ are equal to zero. Our system uses elliptically polarized light, in which there is a phase difference δ between the *s* and *p* electric fields:[17]

$$\delta = \xi_s - \xi_p.$$

When the light is reflected off a surface, this phase difference δ changes, as well as $E_{0,p}$ and $E_{0,s}$.

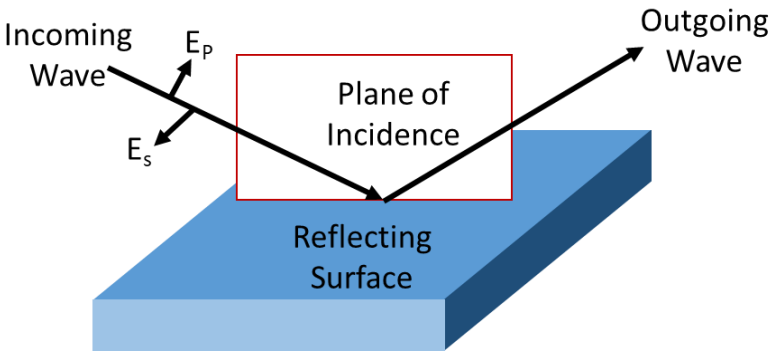

Figure 2.1: Illustration of the plane of incidence relative to the reflecting surface. Note that E_p and E_s are perpendicular to each other as well as the path of light travel, where E_p is in the plane of incidence, and E_s is perpendicular to it.

The ellipsometer consists of a broad spectrum visible lamp emitting unpolarized light, which is then linearly polarized by a polarizer. This light is then turned into elliptically polarized light by a rotating quarter wave plate called the compensator. After reflecting off the sample, the light goes through the analyzer, another polarizer, that turns it into linearly polarized light measured by the detector. The detector is a charge-coupled device (CCD) array that measures the amplitude of the *s* and *p* polarized light intensity at all wavelengths, as well as the phase difference between them. A diagram of our ellipsometer is shown in Figure 2.2.

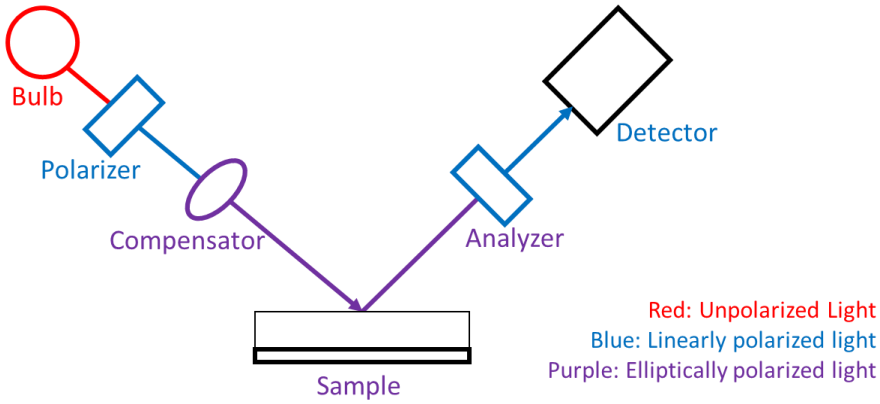

Figure 2.2: Illustration of the various components of our ellipsometer, where the red section represents where the light is unpolarized, the blue section represent where the light is linearly polarized, and the purple sections represent where the light is elliptically polarized.

When light goes from one medium to another with a different index of refraction, as is the case in our system shown in Figure. 2.3, some of the light is reflected from the surface, while some of it is refracted and transmitted through it.

Our samples consist of a silicon substrate covered by a native silicon oxide (SiOx) layer, both of which have a known index and thickness. On top of the SiOx layer is our polymer film, and above the film is air. The silicon substrate has an effectively infinite thickness, where all non-reflected light is absorbed. The index of transparent materials is real, while that of absorbing materials is complex. This sample geometry is shown in Figure 2.3.

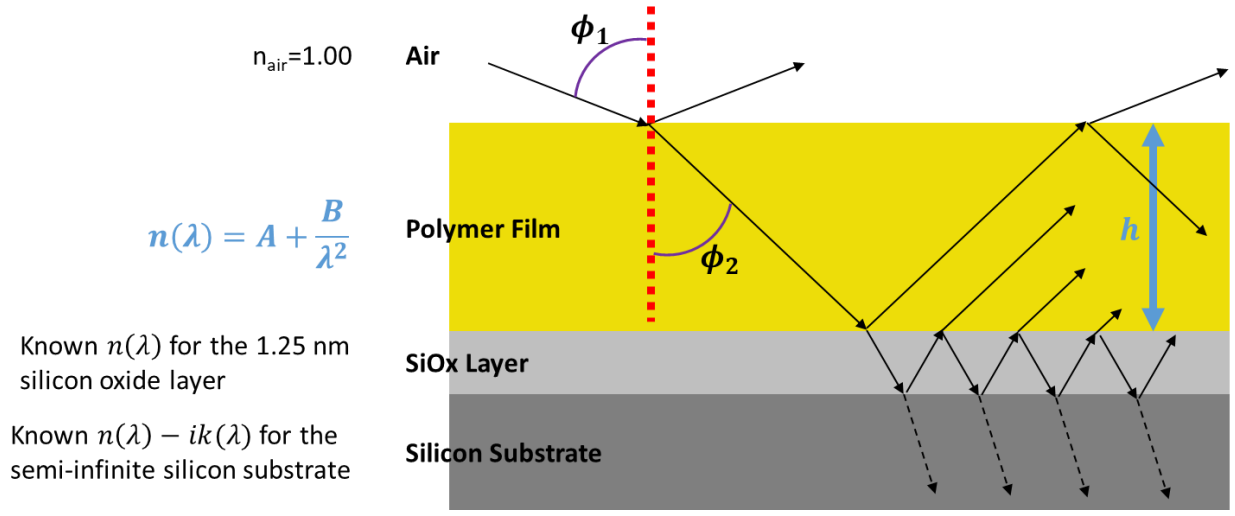

Figure 2.3: Illustration of the optical layer model for our sample geometry. Everything except for *n(λ)* and *h* of the polymer film are known. Due to the small size of the SiO_x layer, this illustration of the light as a ray reflecting within the layer is not accurate.

The Fresnel reflection coefficients r^s and r^p are the ratios of the reflected amplitudes of the incoming *s* and *p* polarized electric fields to those of their incoming incident electric field at that interface. We will use the subscripts to refer to which material the property applies to, where the first material is air and the second material is the polymer film. Using this notation, the Fresnel reflection coefficients can be calculated via the angle of incidence ϕ_1, the angle of refraction ϕ_2, and the refractive indices n_1 and n_2 as:[17]

$$r_{12}^p = \frac{n_2(\lambda)\,cos(\phi_1) - n_1(\lambda)cos(\phi_2)}{n_2(\lambda)\,cos(\phi_1) + n_1(\lambda)cos(\phi_2)} \qquad r_{12}^s = \frac{n_1(\lambda)\,cos(\phi_1) - n_2(\lambda)cos(\phi_2)}{n_1(\lambda)\,cos(\phi_1) + n_2(\lambda)cos(\phi_2)}.$$

The light then reaches the polymer/silicon oxide interface, where the same mechanism occurs again. The silicon oxide layer has a very well characterised index and height. We will ignore the silicon oxide layer in this explanation for the sake of simplicity. The next interface that the light reaches is the silicon substrate interface. The substrate will either reflect or absorb the light. The light that is reflected off the silicon substrate into the polymer will then reach the

polymer/air interface, where some will be transmitted and some will be reflected. This reflection continues until all the light is either absorbed by the subtrate or reflected off of the sample. The total reflection coefficient r_{tot} for all these layers combined is given by the equations:[17]

$$r_{tot}^{p} = \frac{r_{12}^{p} + r_{23}^{p}\exp(-i2\beta)}{1 + r_{12}^{p} r_{23}^{p}\exp(-i2\beta)} \qquad r_{tot}^{s} = \frac{r_{12}^{s} + r_{23}^{s}\exp(-i2\beta)}{1 + r_{12}^{s} r_{23}^{s}\exp(-i2\beta)},$$

where the parameter β is the film phase thickness defined as

$$\beta = 2\pi\left(\frac{h}{\lambda}\right) n_2 \cos(\phi_2),$$

where h is the thickness of the film and λ is the wavelength of the electromagnetic wave.

The ellipsometer collects two sets of data when measuring a sample: Ψ and Δ. When the light bounces off the sample, the phase difference between the parallel and perpendicular polarized light changes from δ_1 of the incident light to δ_2 of the reflected light. This change in phase difference, an angle between 0° and 360°, is called Δ where[17]

$$\Delta = \delta_1 - \delta_2.$$

Ψ is an angle between 0° and 90° that is related to the ratio of the reflectance of the two components of the polarized light. The intensity of light is proportional to the square of the amplitude of the electric field, so the ellipsometer is effectively measuring the tangent of the square root of the ratio of the amplitudes of the *s* and *p* electric fields. This Ψ is defined as:[17]

$$\tan(\Psi) = \frac{|r_{tot}^{p}|}{|r_{tot}^{s}|}.$$

The fundamental equation of ellipsometry, to which our data is fit, defines the complex number ρ such that[17]

$$\rho = \frac{r_{tot}^{p}}{r_{tot}^{s}} = \tan(\Psi)\, e^{i\Delta}.$$

For fitting purposes, we will model the wavelength dependence of the polymer film's refractive index using the Cauchy equation[17,18]

$$n(\lambda) = A + \frac{B}{\lambda^2}$$

where *A* and *B* are fitting parameters and λ is the wavelength of light in microns.[18]

Using these equations and initial 'guess' values of *A*, *B*, and *h* we create a model of the wavelength dependence of Ψ and Δ, and then change these values in such a way to minimize the mean squared error (MSE) which represents the distance between the modeled values of Ψ and Δ and their measured values. The final values of *h*, *A*, and *B* are those which produce a model that most closely resembled the experimental data as shown in Figure 2.4.

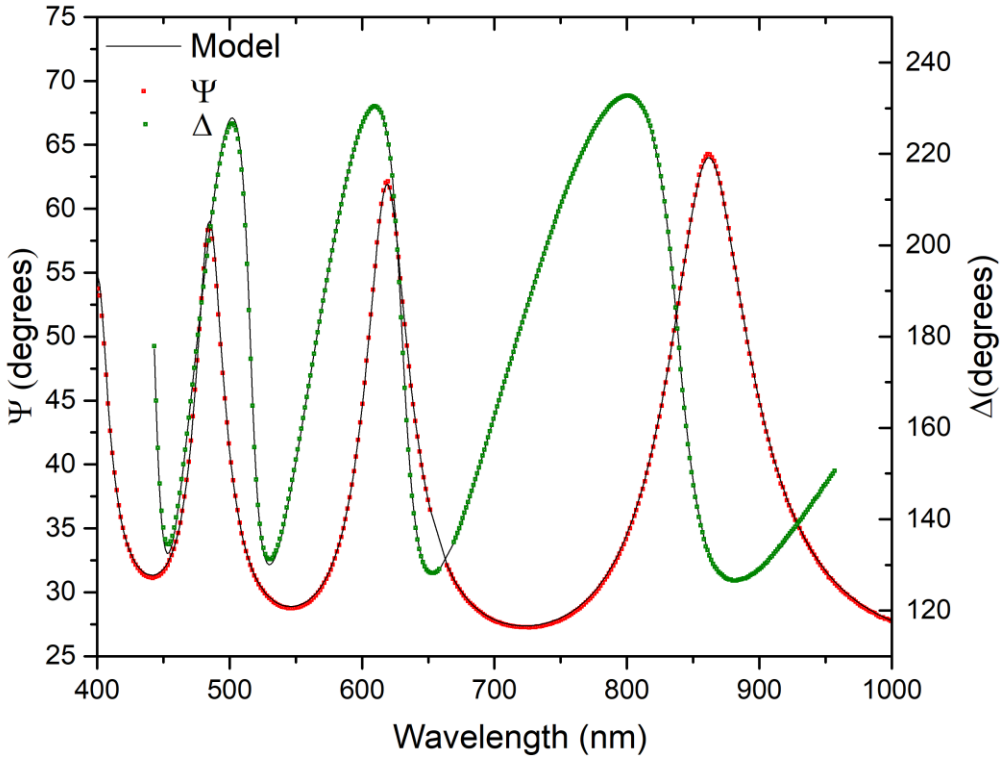

Figure 2.4: Comparison of experimental data (colored points) from an ellipsometry measurement of B-72 showing Ψ and Δ compared to the model to which it was fit (lines), using h = 911 nm, A = 1.439 and B = 0.00399 with a minimized MSE of six.

Ellipsometry will allow the polymers' index and thickenesses to be measured. Furthermore by heating the stage on which the samples sit, the temperature can be varied while also measuing their index and thickness at the same time. This will allow us to determine the properties which were discussed in chapter 1.

Chapter 3: Experimental Methods

3.1: Sample Preparation

Samples consisted of different polymers on top of approximately 2 cm x 2 cm silicon wafers with a 1.25 nm thick native oxide layer. Rohm and Haas, now a subsidiary of the Dow Chemical Company, produced all the polymers we used in this study. The polymers were provided by the Parsons Conservation Lab at Emory University's Michael C. Carlos Museum.

In order to achieve the sample geometry described in Figure 2.3, A-11 samples were spin coated from 10% solutions in toluene onto silicon wafers. While acetone is commonly used in art conservation as the solvent for solutions used as an adhesive, its low boiling point and fast evaporation rate cause it to create uneven samples when spin coating. By using toluene we were able to create more uniform samples. B-72 samples were spin coated onto silicon wafers from 10% solutions in toluene. B-48 does not fully dissolve in toluene, leaving a cloudy solution even after several days. In order to have a homogeneous solution, a small amount of acetone was added in a 1 part acetone to 8 part toluene mixture. We also tried using methyl ethyl ketone (MEK) instead of acetone with 1 part MEK to 6 parts of toluene. Our B-44 samples were spin coated onto silicon wafers from 10% solutions in toluene. The polymer film thicknesses of all the films were between 800 and 1200 nm.

After spin coating all samples were annealed under vacuum at 90 °C for 18-22 hours before their subsequent measurement. In order to control for the possibility that not all of the solvent evaporated from A-11 because of its high T_g (100 °C), additional measurements where the samples were annealed at 120 ^oC for 18 h were performed by Olivia Boyd.

3.2: Measuring refractive index with ellipsometry

At the start of this project the refractive index of B-72 we were measuring at the typical angle of incidence of 65° was found to be consistently higher than the values of index reported in the literature.[1] We found that by changing the angle of incidence, value of the index of refraction measured also varied, as shown in Figure 3.1. The measured index was closest to the literature values of index when a measurement angle of 55° was used. This angle is used throughout the rest of this study.

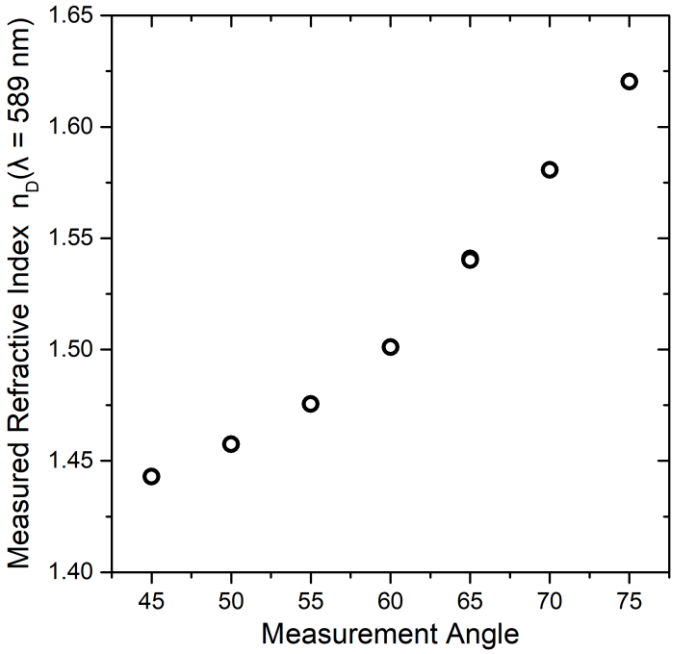

Figure 3.1: Graph of the measured index of refraction at T = 30 °C of a B-72 sample as a function of the angle of incidence of the light beam on the sample.

This angle dependence on the measured index was surprising, so we repeated this test with a sample consisting of 1000 nm of silicon oxide (SiO_x) atop an effectively infinite silicon substrate. As shown in Figure 3.2, an angle dependence of measured index was still found, allowing us to conclude that our polymer does not cause the angle dependence.

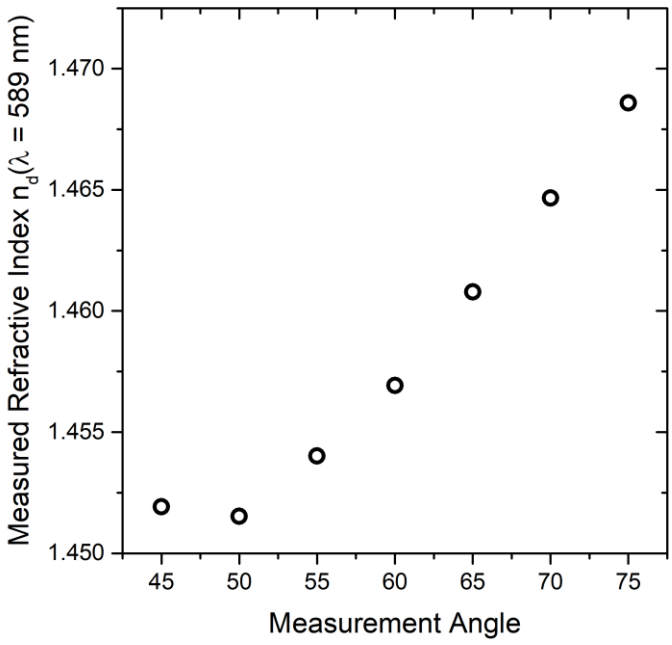

Figure 3.2: Graph of the measured index of refraction at T = 30 °C of a 1000 nm SiO_x sample as a function of the angle of incidence of the light beam on the sample.

After taking measurements, we found that there was a relatively large sample-to-sample variability in the absolute value of the measured refractive index. The height of the stage of the ellipsometer can move up and down in order to accommodate different sized samples. Ideally, our sample would always be parallel with the rest of the ellipsometer, which is accomplished during alignment in which the sample stage is tilted such that the light beam reflecting off the sample falls in the center of the CCD array. Occasionally the sample would be aligned while the height was off causing it to be tilted when the light beam was reflected into the center of the detector. By varying the height of the ellipsometer stage, realigning the sample, and measuring it, we found that different initial conditions in the height of the ellipsometer stage when aligning accounted for the variability in the refractive index data we saw, as shown in Figure 3.2. While the alignment conditions do account for the measurement to measurement variability, the scale in

variability seen is significantly smaller than the measurement angle of incidence dependence of the refractive index previously discussed, and so cannot be used to explain the Figure 3.1.

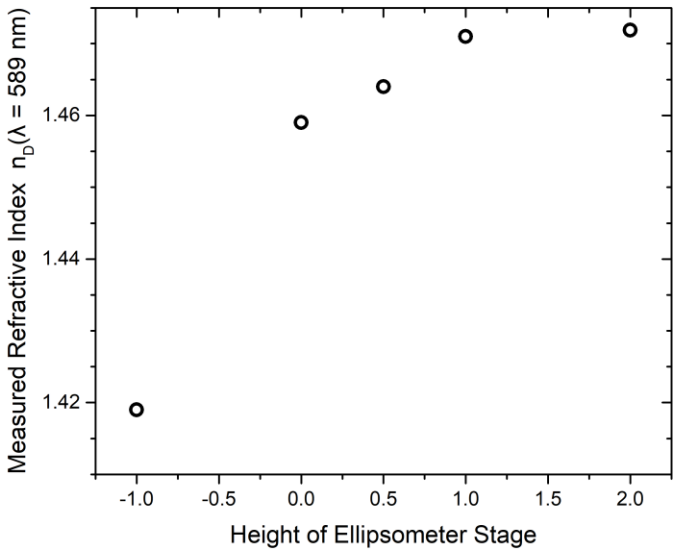

Figure. 3.3: Graph showing how the refractive index of the film measured varying the height at which the sample was aligned before measurement was changed.

3.3: Glass Transition Temperature (T_g) Measurements with Ellipsometry

Ellipsometry measurements were performed with a Woollam M2000 spectroscopic ellipsometer equipped with an Instec HSC 302 temperature stage. There were two temperature profiles used to measure the glass transition temperature. In the first one, samples were heated to 150 °C in 1 minute, held at that temperature for 20 minutes, and then the temperature was decreased to 0 °C in 150 minutes, which results in a cooling rate of 1 ^{o}C/min. The second one, which we used in order to verify there was no degradation of the B-72 caused by bringing it to an elevated temperature, consisted of heating the sample to 80 ^{o}C in 1 minute, keeping it at that temperature for 20 minutes, before cooling down to 0 ^{o}C at 1 ^{o}C/min. Nitrogen gas was flowed at

1.6 L/min over the sample throughout all of the measurements. Data were collected for 5 s every 10 s on cooling.

Ellipsometry measurements of Ψ(λ) and Δ(λ) were fit to a Cauchy model for λ = 400-1000 nm in Woolam's CompleteEASE software using the "PS_Aging" model with the native oxide layer held constant at 1.25 nm. Index of refraction was determined using the Cauchy model where the wavelength dependence is defined as $n(\lambda) = A + \frac{B}{\lambda^2}$. Our indices are reported at λ = 589 nm, which corresponds to the yellow doublet D-line of sodium and is the commonly used wavelength for reporting in art conservation.[1] Glass transition temperatures were found by doing a linear fit of thickness *h*(*T*) data before and after the glass transition, and finding their intersection. For comparison purposes, *h*(*T*) were normalized at *h*(130 °C). Thermal expansion was calculated by taking the numerical derivative of the thickness as a function of height where Δ*T* is 4.2 °C and *h*(130 °C) is the thickness of the sample at 130 °C, and $h\left(T \pm \frac{\Delta T}{2}\right)$ is the thickness of the sample at that temperature.[9]

$$\alpha(T) = \frac{h\left(T + \frac{\Delta T}{2}\right) - h\left(T - \frac{\Delta T}{2}\right)}{h(130\ °C)\Delta T}.$$

This ΔT = 4.2 °C was previously shown by Kawana and Jones to give good values of thermal expansivity. As shown in their paper, it is also an effective way to evaluate the glass transition of polymers which do not have a well defined transition.[9]

Chapter 4: Results and Discussion

In this chapter I will be discussing measurements on our four polymers: A-11, B-72, B-48N, and B-44. Samples of these polymer films on silicon were heated to 150 °C (with one exception discussed below) and held there for 20 minutes to allow the polymer to relax before being cooled at 1 °C per minute to 0 °C. Using ellipsometry, as discussed in sections 2 and 3.3, I was able to measure the thickness $h(T)$ and refractive index $n(T)$ of the polymer films as a function of temperature. I will be discussing each polymer individually, comparing them, and then examining mixtures of B-48N and B-72.

4.1: A-11

Three A-11 films with thicknesses 850-950 nm were analyzed as described in section 3.3. The film thickness $h(T)$ as a function of temperature data were normalized by dividing by the thickness of that sample at 130 °C, allowing data to overlap despite the different samples having slightly different thicknesses. A plot of normalized film thickness $h(T)/h(T = 130\ °C)$ as a function of temperature T is shown in Figure 4.1. At high temperatures the film thickness of our samples changes linearly with temperature, which corresponds with when the polymer is in a rubbery state. At low temperatures the film thickness also changes linearly with temperature, with a different slope than in the rubbery state. These temperatures are when the polymer is in a glassy state. The intersection of these two lines is the glass transition temperature T_g, which we measured as 98 ± 2 °C by determining the intersection between the two linear fits above and below the transition. In practice the glass transition temperature does not happen instantly at a given point, but rather has a continuous change in slope over a range in temperatures. In A-11 this transition happens over a limited temperature range.

In order to have an experimental procedure that was identical for all our polymers, A-11 was annealed at 90 °C, chosen because it is a temperature at least 20 °C above the T_g of our other polymers. This meant that the A-11 samples were not being annealed above their T_g for 18-22 h, and the only annealing above T_g occurred on the ellipsometer, at 150 °C for 20 minutes immediately before the start of the measurement. In order to verify that this did not cause any unexpected effects on the measurements, we vacuum annealed two samples at 120 °C overnight prior to measurement, and observed that there is no difference between samples annealed at 120 °C (circles and squares), and the samples annealed at 90 °C (triangles).

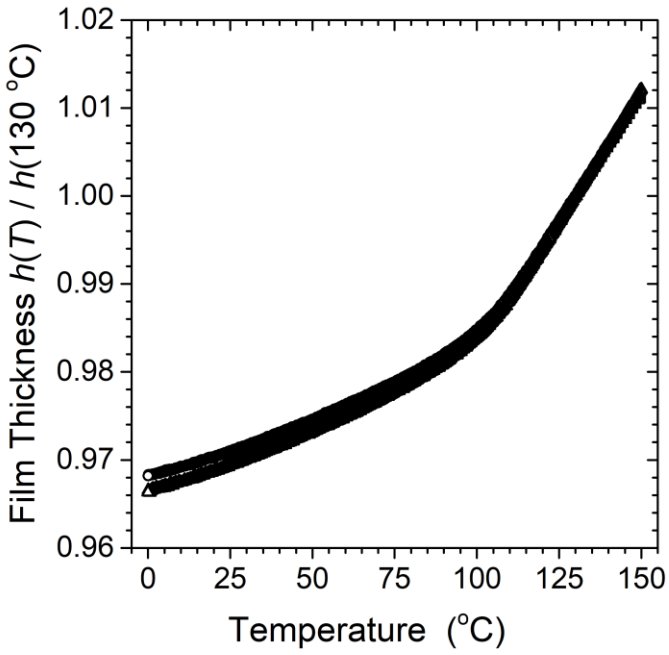

Figure 4.1: Normalized thickness of A-11, normalized at its value at 130 °C, as a function of temperature. Shown are three different samples, one for which h(30 °C) = 874 nm (squares) whose T_g was found to be 100 °C, one for which h(30 °C) = 845 nm (circles) whose T_g was found to be 98 °C, and one for which h(30 °C) = 930 nm whose T_g was found to be 97 °C (triangles)

In order to better visualize the breadth of the glass transition, I took the numerical derivative of the film thickness (as described in section 3.3) and studied it as a function of

temperature, shown in Figure 4.2. Above 115 °C the thermal expansivity is constant, at which point it starts decreasing rapidly with decreasing temperature, and appears to stabilize at 80 °C.

Even as we approach 0 °C the thermal expansivity does not appear to be constant. This relatively constant thermal expansivity below 80 °C means that objects conserved with A-11 will be fairly stable even if the objects are exposed to high temperatures. For example the objects excavated from the site of Troy as described by Strahan and Korolnik[5] would have a relatively constant thermal expansivity if they were adhered with A-11 despite the large temperature fluctuations; this constant thermal expansivity is important for the stability of the joint. However, when used as an adhesive in art conservation, where the polymer cannot be annealed at high temperatures, the solvent will have evaporated without having allowed the polymer to relax, forcing it to stay in a less dense and more porous state, making it brittle as is commonly observed art conservation.[1,10]

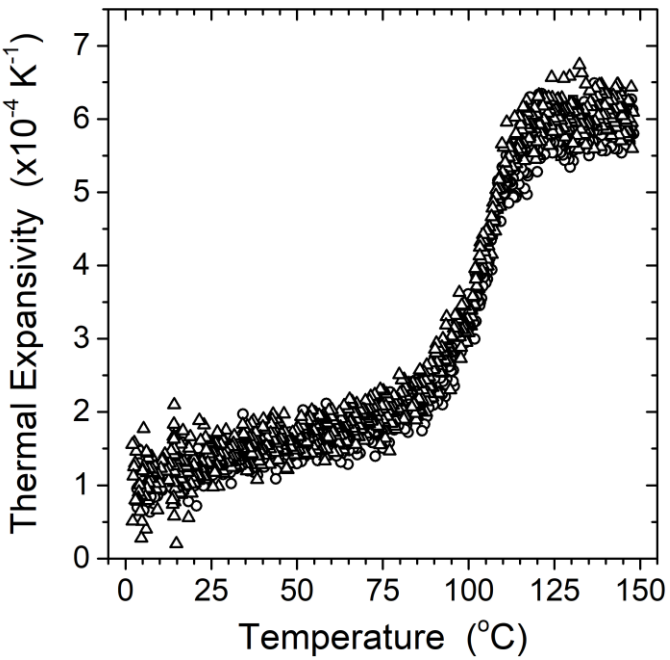

Figure 4.2: Thermal expansivity of A-11 as a function of temperature. Shown are three different samples, one for which *h*(30 °C) = 874 nm (squares), one for which *h*(30 °C) = 845 nm (circles), and one for which *h*(30 °C) = 930 nm (triangles).

The index of refraction, as shown in Figure 4.3, presents some slight variation that is caused by small differences in the initial alignment conditions of the ellipsometer. Based on the average of three samples at 30 °C, we measured an index of refraction of 1.479 ± 0.003 with *A* values of 1.46 ± 0.05 and *B* values of 0.00441 ± 0.00005 μm^2 at 30 °C. This index is within the error of the literature reported values of index.[1]

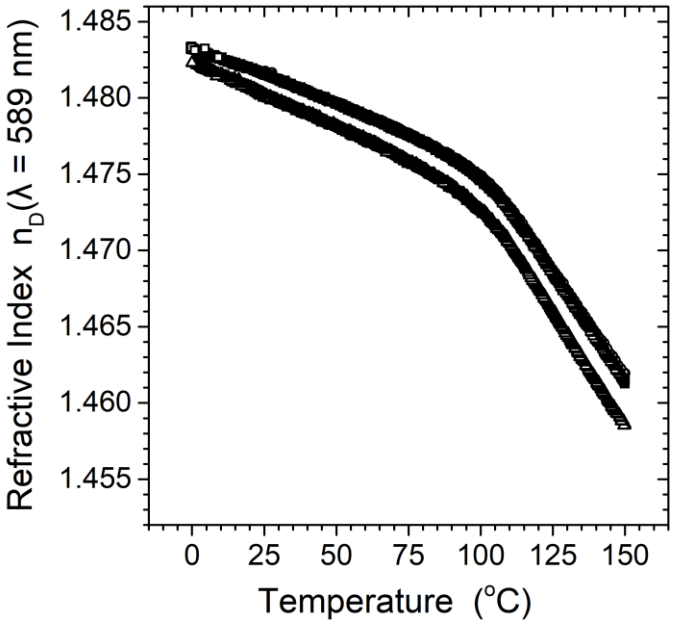

Figure 4.3: Refractive index of A-11 as a function of temperature. Shown are three different samples, one for which *h*(30 °C) = 874 nm (squares), one for which *h*(30 °C) = 845 nm (circles), and one for which *h*(30 °C) = 930 nm (triangles).

These measurements of A-11 match the literature[1] data and what we expect from a polymer consisting of pure methyl methacrylate units. These results showed that the properties

we were calculated were the actual film properties and gave confidence in the following measurements.

4.2: B-72:

Five B-72 films with thicknesses between 870 nm and 1020 nm were analyzed as described in section 3.3. Measured T_g values were 39 ± 2 °C based on an average of the five samples. A plot of normalized film thickness $h(T)/h(T = 130\ °C)$ as a function of temperature T is shown in Figure 4.4.

The low T_g of B-72 might cause it to undergo thermal degradation when being annealed at 150 °C on the ellipsometer. In order to assuage this concern, I measured one film which was never brought significantly over T_g in order to make sure that the polymer did not undergo thermal degradation caused by bringing it to 150 °C. This film was annealed overnight at 60 °C, and measured on the ellipsometer starting at 60 °C. The thickness of this shorter run was normalized by its thickness at T = 60 °C, and then shifted to match the normalized thickness at 60 °C of the other runs that were normalized at 130 °C, by subtracting their difference in normalized thickness at that temperature which was 0.0425. The measured T_g value of these low temperature runs is 34 ± 1 °C. This is significantly lower than the T_g of the measurements following our standard annealing and measurement procedure for which T_g = 40 ± 2 °C. Closer observation reveals that these low temperature samples have a slightly lower measured T_g based on the standard use of the intersection of linear fits because insufficient data above the transition is available to give a good fit of the rubbery regime. If we use the data of the samples annealed and measured from 150 °C to 0 °C and fit the glassy regime data only in the temperature range

50 °C to 60 °C, instead of in the high temperature range, the data also give a T_g of 34 °C ± 1 °C, which agrees with the T_g of the samples not annealed at a high temperature. This suggests that there is no polymer degradation happening when B-72 samples are annealed at 150 °C.

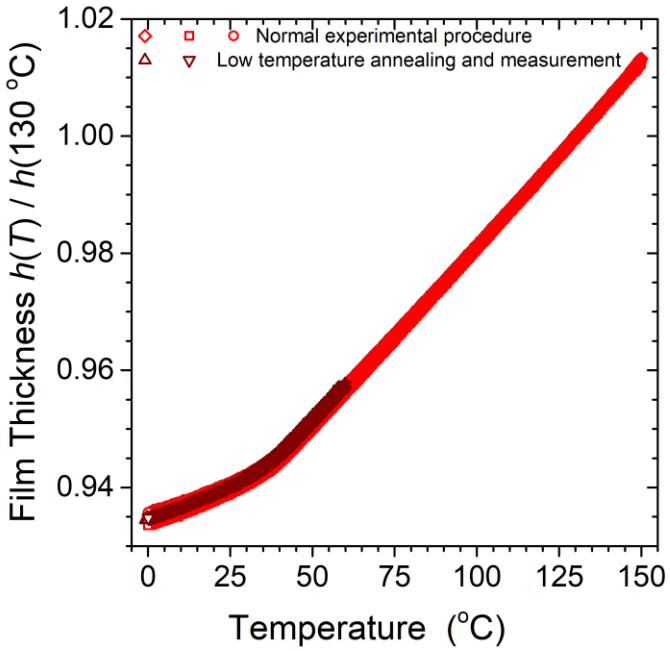

Figure 4.4: Thickness of B-72, normalized by its thickness at 130 °C, as a function of temperature. The circles (h(30 °C) = 881 nm, T_g = 40 °C), squares (h(30 °C) = 924 nm, T_g = 38 °C), and diamonds (h(30 °C) = 870 nm, T_g = 41 °C) are from films spin cast from toluene solutions, annealed at 150 °C for 20 minutes before measurement. The up triangles (h(130 °C) = 1021 nm, T_g = 34 °C) and down triangles (h(130 °C) = 1022 nm, T_g = 33 °C) were annealed at 60 °C for 20 minutes before measurement.

The thermal expansivity found using the numerical derivative of the film thickness as a function of temperature, as described in section 3.3, are shown in Figure 4.5**.** At room temperature the B-72 is almost in the glassy regime, which explains its stability. At this temperature, its glass transition is only just finishing which likely explains why allowing solvent cast B-72 to rest and anneal at room temperature allows some of the stresses to relax leading to a less brittle material. This also means that even slight increases in temperature would quickly

bring the polymer to a state where it can relax more of its stresses. For example, heating it up to 35 °C would likely allow much quicker solvent evaporation and better adhesive strength, although this is often impractical for conservation situations.

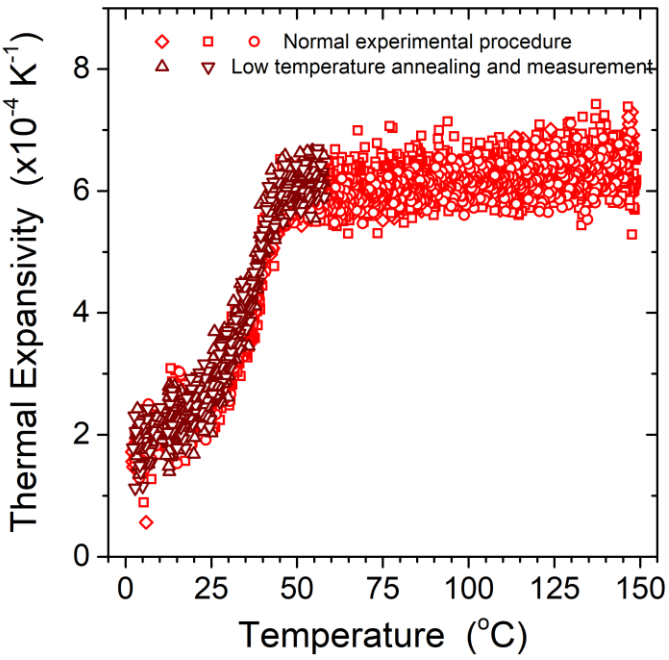

Figure 4.5: Thermal expansivity of B-72 as a function of temperature. Shown are five different samples, one for which *h*(130 °C) = 924 nm (squares), one for which *h*(130 °C) = 881 nm (circles), one for which *h*(130 °C) = 930 nm (diamonds), one for which *h*(130 °C) = 1021 nm (up triangles) and one for which *h*(130 °C) = 1022 nm (down triangles).

The index of refraction shown in Figure 4.6 presents some slight variation that is caused by differences in the initial alignment conditions of the ellipsometer. We measured an index of refraction at 30 °C of 1.460 ± 0.003. The *A* value of our films were 1.457 ± 0.009 at 30 °C and the *B* values of our films were 0.0044 ± 0.0005 μm^2 at 30 °C.

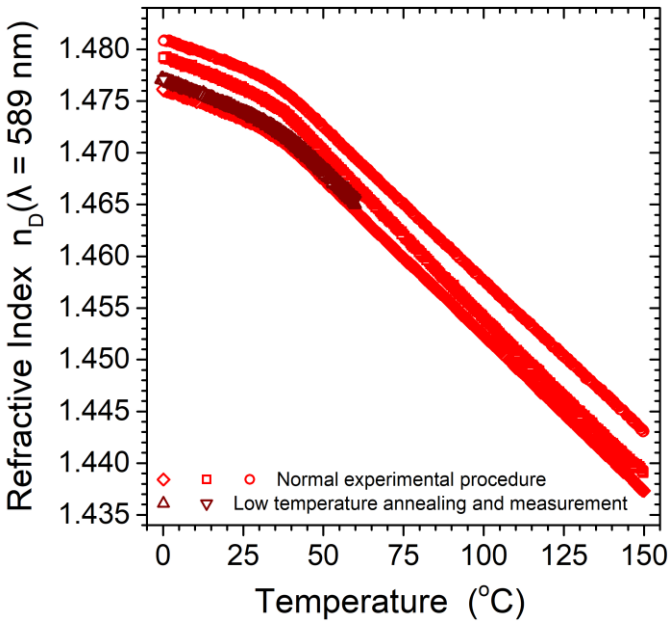

Figure 4.6: Index of B-72 as a function of temperature. Shown are five different samples, one for which *h*(130 °C) = 924 nm (squares), one for which *h*(130 °C) = 881 (circles), one for which *h*(130 °C) = 930 nm (diamonds), one for which *h*(130 °C) = 1021 nm (up triangles) and one for which *h*(130 °C) =1022 nm (down triangles).

4.3: B-48N

The B-48N films with thicknesses between 880 nm and 940 nm were analyzed as described in section 2.2. The measured T_g values are 39 ± 2 °C. A plot of normalized film thickness $h(T)/h(T = 130\ °C)$ as a function of temperature T is shown in Figure 4.7. We also examined if there was an effect based on what solvent the film was spin coated from, and found no difference between films cast from a mixture of toluene and methyl ethyl ketone (MEK) and a mixture of toluene and acetone. Toluene was used in both cases because its high boiling point makes it easy to spin coat from, while the acetone or MEK was added because B-48N is not fully soluble in toluene.

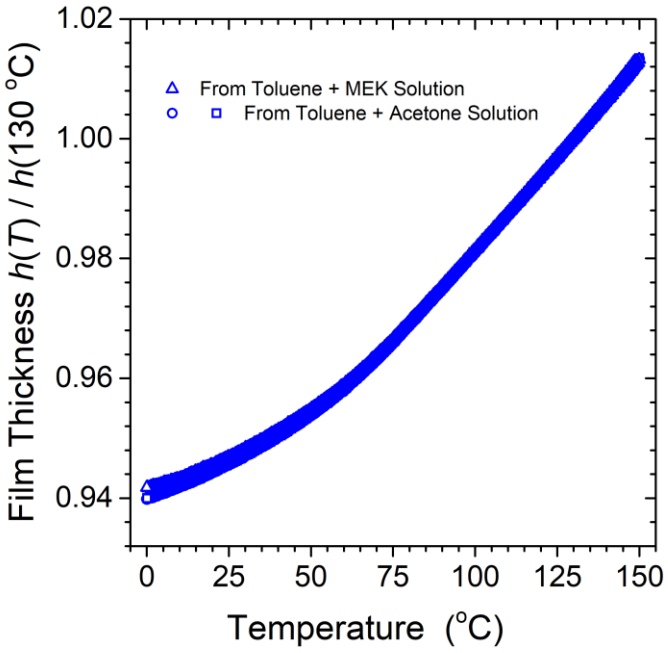

Figure 4.7: Normalized thickness of B-48N, normalized at its value at 130 °C, as a function of temperature. Shown are three different samples, one for which h(30 °C) = 893 nm (squares) whose T_g was found to be 55 °C, one for which h(30 °C) = 889 nm (circles) whose T_g was found to be 56 °C, and one for which h(30 °C) = 939 nm whose T_g was found to be 56 °C (triangles)

The thermal expansivity, found using the numerical derivative of the thickness as a function of temperature, as described in section 3.3, are shown in Figure 4.8**.** The transition is still happening below room temperature, through the entire range that was studied. This means that any small temperature variations will drastically affect the dynamics of the polymer.

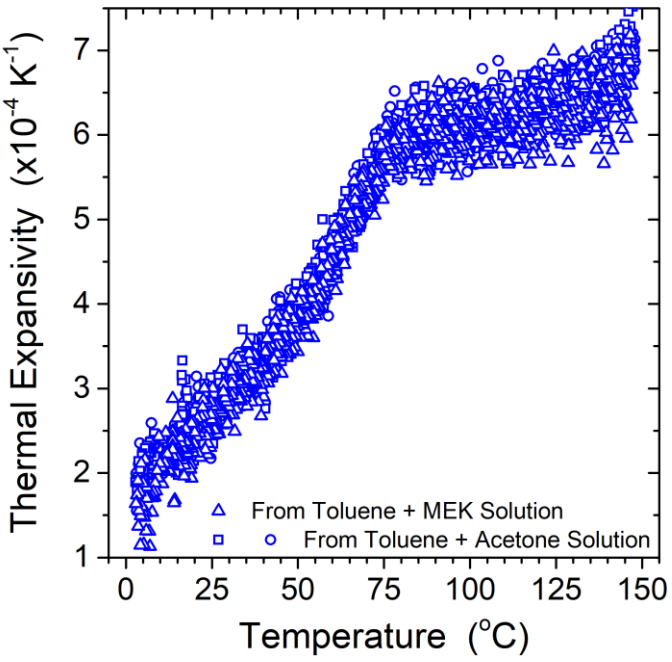

Figure 4.8: Thermal expansivity of B-48N as a function of temperature. Shown are three different samples, one for which *h*(30 °C) = 893 nm (squares), one for which *h*(30 °C) = 889 nm (circles), and one for which *h*(30 °C) = 939 nm (triangles).

The index of refraction, as shown in Figure 4.9, presents some slight variation, which is caused by differences in the initial alignment conditions of the ellipsometer. We measured an index of refraction at 30 °C of 1.4787 ± 0.0009. The *A* value of our films were 1.4658 ± 0.0008 at 30 °C. The *B* values of our films were 0.00449 ± 0.00004 μm^2 at 30 °C. There was no significant difference in the refractive index if it was cast from a toluene and MEK solution compared to when it was cast from a toluene and acetone solution.

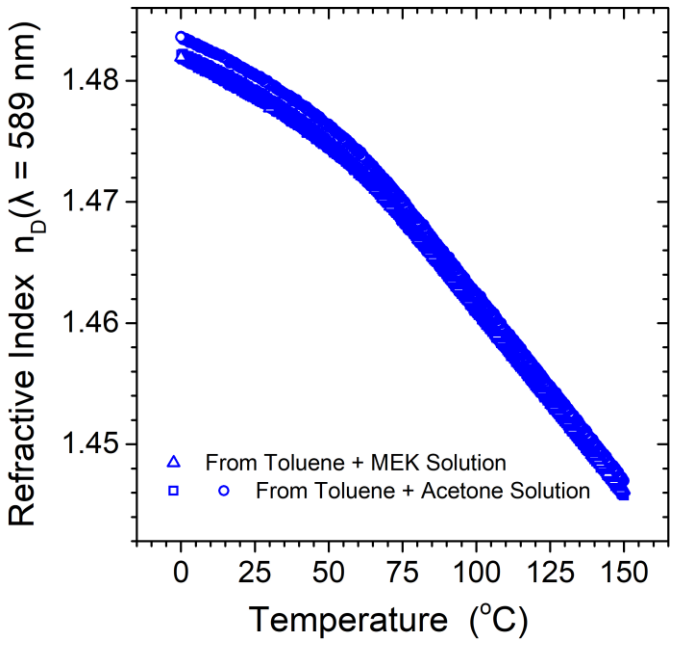

Figure 4.9: Index of B-48N as a function of temperature. Shown are three different samples, one which h(30 °C) = 893 nm (squares), one which h(30 °C) = 889 nm (circles), and one which h(30 °C) = 939 nm (triangles).

4.4: B-44

The B-44 films with thicknesses between 900 and 920 nm were analyzed as described in section 2.2. These samples were made and measured by Olivia Boyd, and analyzed by me. The measured T_g values are 56 ± 1 °C. A plot of normalized film thickness $h(T)/h(T = 130$ °C) as a function of temperature T is shown in Figure 4.10.

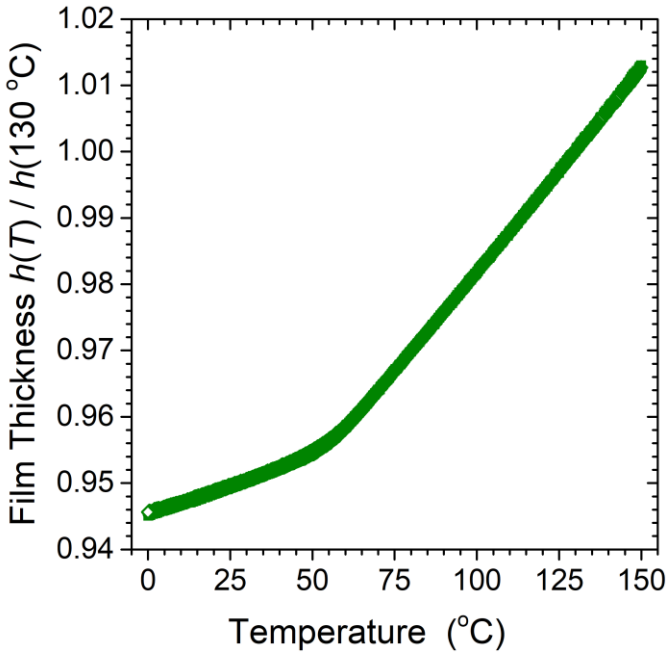

Figure 4.10: Normalized thickness of B-44 as a function of temperature. Shown are three different samples, one for which h(130 °C) = 916 nm and T_g = 57 °C (squares), one for which h(130 °C) = 919 nm and T_g = 55 °C (circles), and one for which h(130 °C) = 909 nm and T_g = 57 °C (diamonds).

The thermal expansivity, found using the numerical derivative of the thickness as a function of temperature, as described in section 2.2, are shown in Figure 4.11. The transition occurs relatively rapidly starting at around 45 °C and continuing to around 70 °C. This means that unless the polymer is heated into or above that temperature range, annealing will have a negligible effect.

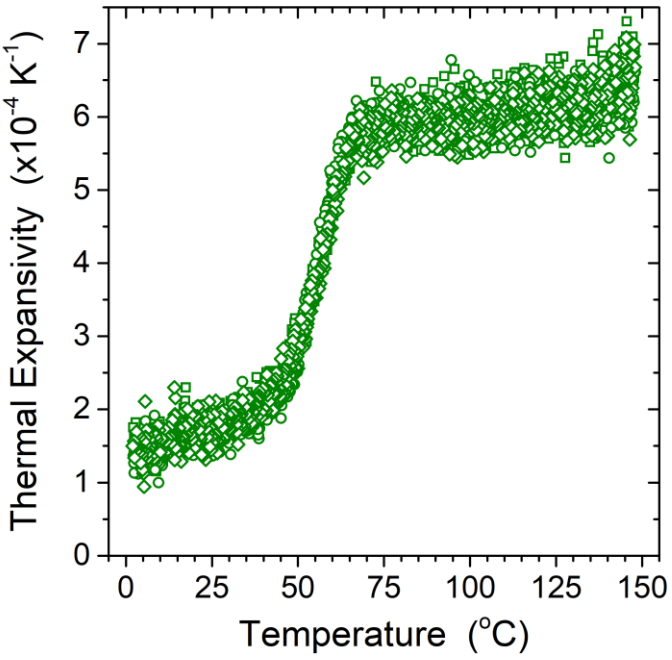

Figure 4.11: Thermal expansivity of B-44 as a function of temperature. Shown are three different samples, one for which *h*(130 °C) = 916 nm (squares), one for which *h*(130 °C) = 919 nm (circles), and one for which *h*(130 °C)= 909 nm (diamonds).

The index of refraction, as shown in Figure 4.12, presents some slight variation, which is caused by differences in the initial alignment conditions of the ellipsometer. We measured a room index of refraction of 1.477 ± 0.003. The *A* value of our films were 1.463 ± 0.003 at 30 °C. The *B* values of our films were 0.0048 ± 0.0001 μm^2 at 30 °C.

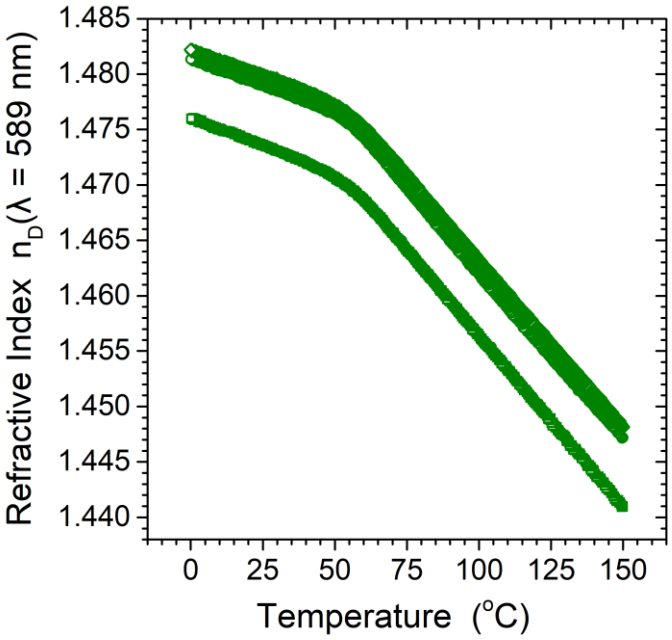

Figure 4.12: Index of B-44 as a function of temperature. Shown are three different samples, one for which *h*(130 °C) = 916 nm (squares), one for which *h*(130 °C) = 919 nm (circles), and one for which *h*(130 °C) = 909 nm (diamonds).

4.5: Comparison of the pure polymers

Our measured T_g of A-11, B-72, and B-44 agree with those reported in the literature.[1] The measured T_g of B-48N is higher than that commonly found in the literature.[1] The T_g in the literature is often measured using differential scanning calorimetry (DSC).[1] Our measured B-48N T_g which is higher than the literature is likely due to the fact that the glass transition has not fully completed by the time the polymer is at 0 °C, leading to an artificially elevated T_g fit, due to an inability to properly fit a straight line in the glassy regime. Using a temperature profile that goes down to -20 °C would be useful for accurate measurements in future studies of B-48N. However, this is problematic with ellipsometry as water vapor in the atmosphere begins condensing on the sample, obscuring the beam path, despite the dry nitrogen flowing over it.

A comparison of the normalized film thickness $h(T)/h(T = 130\ °C)$ as a function of temperature T of each of our polymers is shown in Figure 4.13. We can see that, on cooling, A-11 falls out of the rubbery state first, while B-44 appears to become a glass next, then B-48N, and B-72. Especially with the last three of those polymers, however, it can be difficult to analyze their differences using this plot because there is a lot of overlap between them.

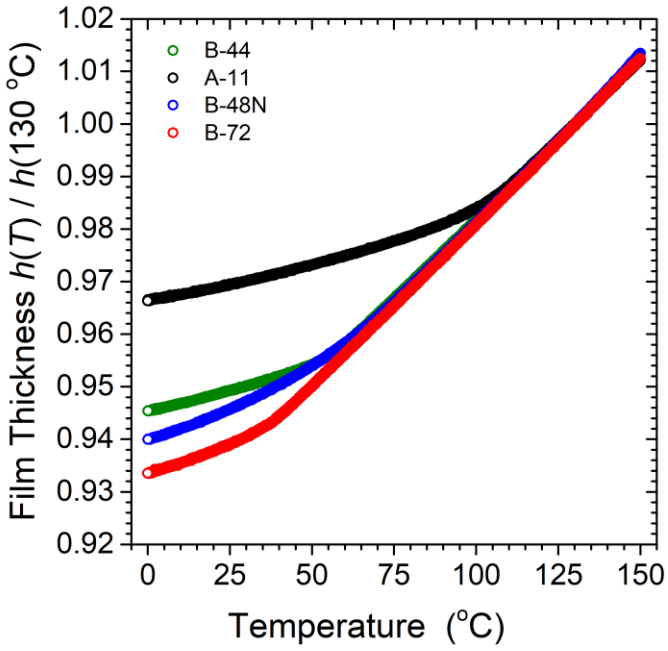

Figure 4.13: Normalized film thickness as a function of temperature of all our polymers.

In order to better examine the differences between our polymers, we will look at the thermal expansivity as a function of temperature. We can see that the B-72 glass transition has a fairly small breadth, starting at 50 °C and ending at 15 °C, happening over 35 °C. B-44 has a very similar transition at a slightly higher temperature, with the transition spanning 25 °C from when it starts at 65 °C to when it ends at 40 °C. A-11 also has a transition with a breadth of approximately 35 °C, starting at 120 °C and ending by the time it reaches 85 °C. B-48N is

significantly different from these polymers in the breadth of its transition; the transition starts at 75 °C, which is higher than both B-44 and B-72, but does not complete until it is at 0 °C, significantly lower than the B-44 and B-72 do.

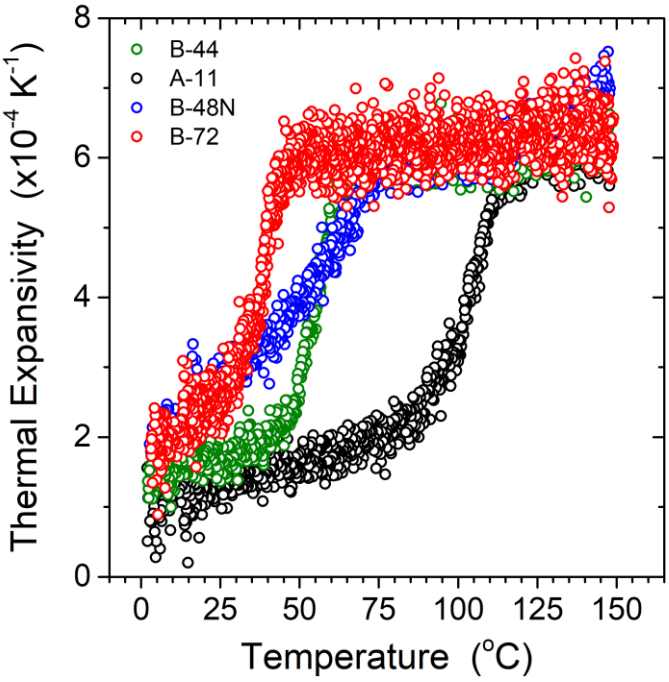

Figure 4.14: Thermal expansivity of our polymers as a function of temperature.

In order to better interpret this data, we smoothed it using the locally weighted scatterplot smoothing (LOWESS) method in the OriginLab data processing. This method uses a weighted regression function, where data surrounding each data point is fit to a linear function. This method uses a weighting function that gives more importance to the data points closest to the point being smoothed, and less to those further out. This allows each datum to be smoothed using a large amount of surrounding data, without losing non-linear aspects, which occur at the glass transition. In our case, we will call the distance in the x axis from the datum being smoothed to

the furthest datum being used to smooth is d_i. The specific weighting function used by this algorithm is:[19]

$$w_i(x) = \left(1 - \left(\frac{|x - x_i|}{d_i}\right)^3\right)^3,$$

where x_i is the point being smoothed. This weighting function is then used to determine the importance of each point used in the linear regression.[19] The smoothing range we used, equal to $2d_i$ was 83 points, equal to 10% of all the data. This range was chosen as it is the range recommended by our data analysis software. This smoothed data is shown in Figure 4.15.

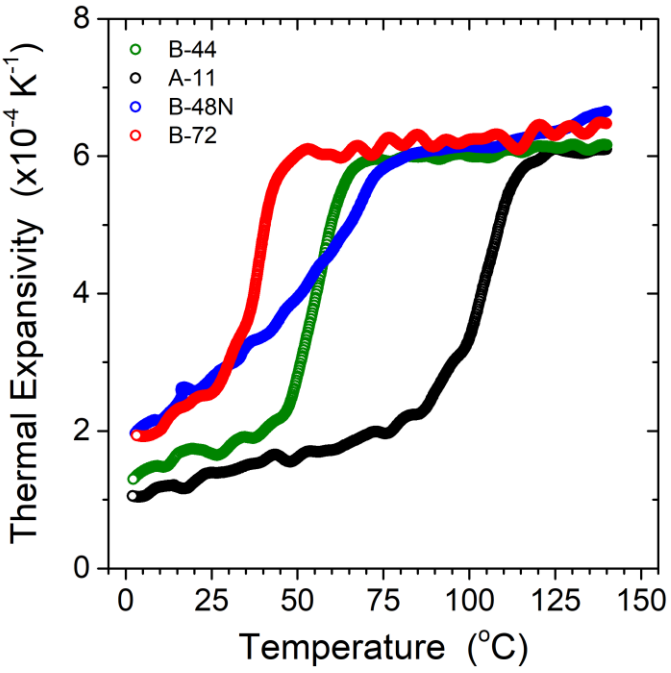

Figure 4.15: Thermal expansivity of our polymers as a function of temperature, where data are smoothed using the LOWESS method.

As discussed in the introduction, the literature values of index for our polymers are equal to 1.480 ± 0.003. The measured refractive indices of our polymers are all within this error,

agreeing with the literature values of index.[1] A comparison of the refractive index as a function of temperature of each of our polymers is shown in Figure 4.15. The small variations in index may also be related to a difference in initial alignment conditions, as discussed in section 3.2.

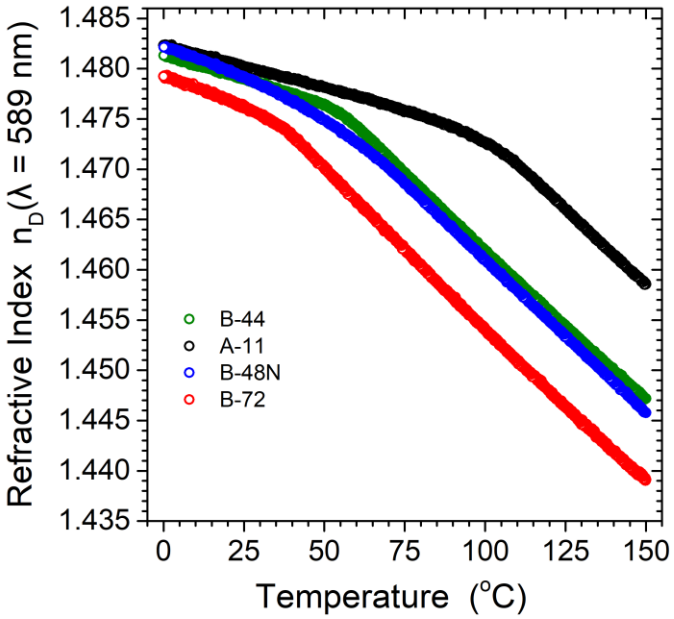

Figure 4.16: Refractive index of our polymers as a function of temperature. While at high temperatures they deviate from each other significantly, at room temperatures they are very similar.

4.6: Mixtures of B-72 and B-48N

When B-72 is used as an adhesive, it has been observed[10] to move of flow over a period of several years in a behavior known as creep. This occurs notably when an object is exposed to higher temperatures than those experienced in a climate-controlled museum. In order to prevent creep, conservators have added a small amount of B-48N to B-72 when reconstructing large ceramic jars that were found at the site of Troy, and would be stored in non-climate controlled conditions.[5] This adhesive was then used in the reconstruction of Tullio Lombardo's *Adam* at the Metropolitan Museum of Art.[6] In her master's thesis[10], Jessica Betz sought to quantify what effect

this mixture had on the mechanical properties of objects conserved with them. She created samples of broken limestone and terracotta that she repaired with each of the polymers described in this study, as well as the mixtures that we will be studying in this section. She then put these samples under a variety of mechanical tests. In the first test, samples were cycled between 30 °C and 60 °C to stress the bond, before subjecting them to a four-point bend flexure test, and examining the failure mode and weight. She also subjected them to a thermally induced creep behavior test, where a constant force was applied to the center of the sample, and the sample was slowly heated up by a UV lamp. The temperature at which it failed, as well as how long it took to fail, was studied. These tests both study the mechanical properties of the polymers. She found that 1:3 and 3:1 mixture of B-72 and B-48N were not significantly different, and that it seemed that the properties of the B-48N seemed to dominate the mixture. She further found that in the creep behavior test the polymers with higher reported T_gs lasted longer and failed at higher temperatures than those with lower T_gs.

In order to further shed light on this subject, using experimental techniques that provide different information, I studied a mixture consisting of one part B-72 and three parts B-48N, as well as one consisting of three parts B-72 and one part B-48N. These 1:3 and 3:1 B-72:B-48N ratios were chosen to match what was studied previously.[10]

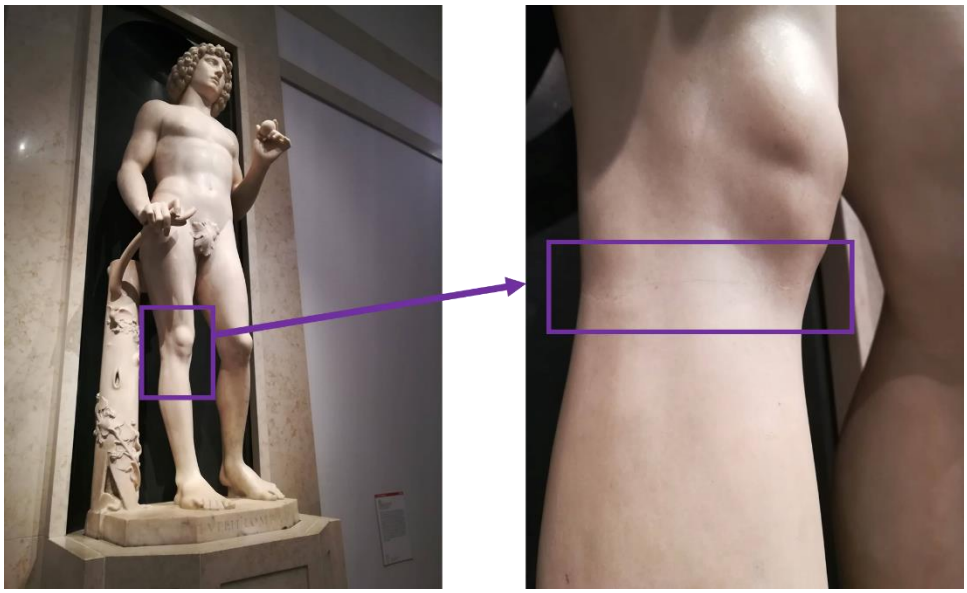

Figure 4.17: Picture of *Adam* by Tullio Lombardo, taken at the Metropolitan Museum of Art. The entire statue is shown on the left, while a close up of one of the joints, repaired with a 3:1 mixture of B-72:B-48N is on the right. I added a purple box around the image of the joint to make it easier to locate.

Films with the 3:1 mixture of B-72 and B-48N with thicknesses between 996 and 1042 nm were analyzed as described in section 2.2. The measured T_g values are on average 44 ± 2 °C. The 1:3 mixtures of B-72 and B-48N with thicknesses between 851 and 859 nm were analyzed as described in section 3.3. The measured T_g values are on average 47.3 ± 0.2 °C. B-72 had an average T_g of 40 °C and B-48N had an average T_g of 55 °C, so the T_g of these mixtures, which are between the two, match with what would be expected. A comparison plot of normalized film thickness $h(T)/h(T = 130\ °C)$ as a function of temperature T is shown in Figure 4.16.

The Fox equation predicts the T_g of polymer mixtures where w_1 and w_2 are the weight fraction of each component of the mixture as:[8]

$$\frac{1}{T_{gmix}} = \frac{w_1}{T_{g2}} + \frac{w_2}{T_{g1}}$$

Using the literature values of T_g for B-72 and B-48 and the Fox equation above, I calculated the T_g of the mixtures as

$$T_g(1{:}3\ B72{:}B48N) = 47.1,$$

and

$$T_g(3{:}1\ B72{:}B48N) = 42.1.$$

These values of T_g match well the values of the 1:3 and 3:1 mixtures of B-72:B-48N which we measured for the different mixtures: 47.3 ± 0.2 °C and 44 ± 2 °C, respectively.

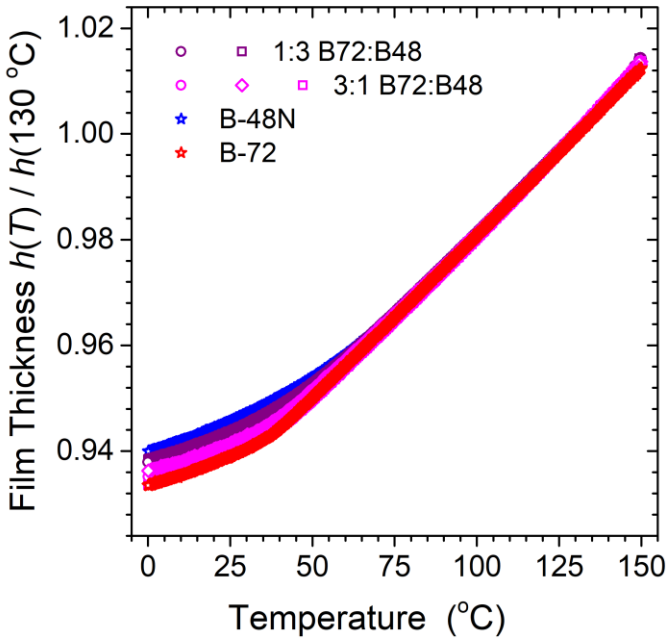

Figure 4.18: Normalized thickness of B-48N and B-72 mixtures as a function of temperature. The pink data, where circles are from a sample with thickness h = 1042 nm and a measured T_g of 45 °C, squares are from a sample with thickness h = 996 nm and a T_g of 45 °C, and the diamonds with thickness h = 1023 nm and a T_g of 42 °C are from samples which consist of a 3:1 mixture of B-72 and B-48. The purple data, where the circles are data from a sample with h = 859 nm and T_g = 47 °C, and the squares are data from a sample with h = 851 nm and T_g = 47 °C are from samples consisting of a 1:3 mixture of B-72 and B-48N. The red data and blue data are representative plots of B-72 and B-48N respectively to allow easier comparison to the pure polymer.

In order to better illustrate the difference in how the samples' film thickness changes with temperature, I examined their thermal expansivity, as shown in Figure 4.17. The addition of B-48N to the B-72 makes the glass transition begin occurring at a higher temperature, but the small breadth of B-72's transition, compared to that of B-48N makes the mixtures' transition finish at a higher temperature. In other words, it seems that at high temperatures it is the behavior of the B-48 that dominates, while at lower temperatures the B-72 appears to have the greatest effect. The 1:3 B-72:B-48N mixture has a glass transition that occurs at a slightly higher temperature, but otherwise goes through the glass transition in the same way as the 3:1 mixture. This suggests that using a 1:3 B72:B48N mixture may be able to provide the same excellent properties as the 3:1 mixture with perhaps a better stability above 40 °C.

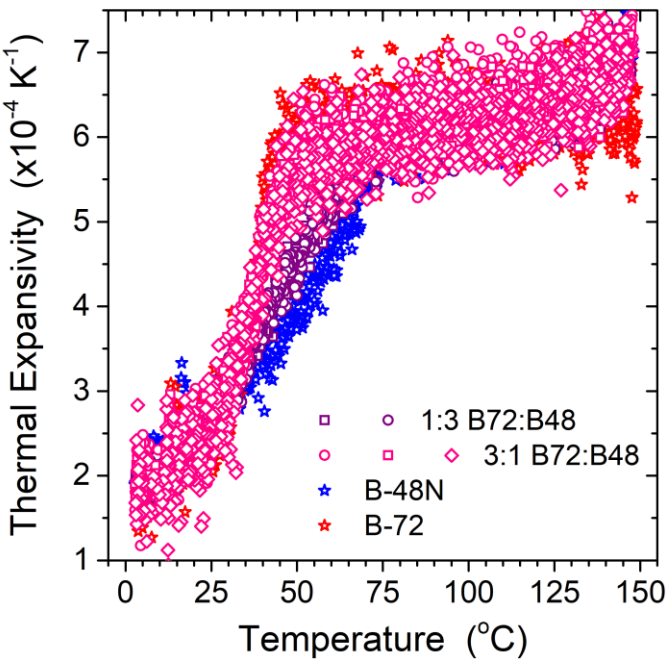

Figure 4.19: Thermal expansivity of B48N and B72 mixtures as a function of temperature. The pink data are from samples consisting of a film of 3:1 mixture of B-72 and B-48 with thickness *h* = 1042 nm (circles), 996 nm (squares), and 1023 nm (diamonds). The purple data are from samples consisting of a film of 1:3 mixture of B-72 and B-48 with a thickness *h* = 859 nm

(squares) and *h* = 851 nm (circles). In order to be able to compare to the pure polymers, also shown are representative data of B-72 (red stars) and B-48N (blue stars).

Due to the amount of noise in the data being on the same scale as the difference between the different mixtures' curves, data were smoothed, as discussed in section 4.5. This data is shown in Figure 4.19 below, and shows that the 3:1 mixture of B-72:B-48N starts its T_g at a slightly higher T_g than the pure B-72, and shares its small breadth of transition. The 1:3 B-72:B-48N mixture has a broader transition due to an onset temperature that is comparable to that of B-48N, however its transition completes before the pure B-48N completes its transition.

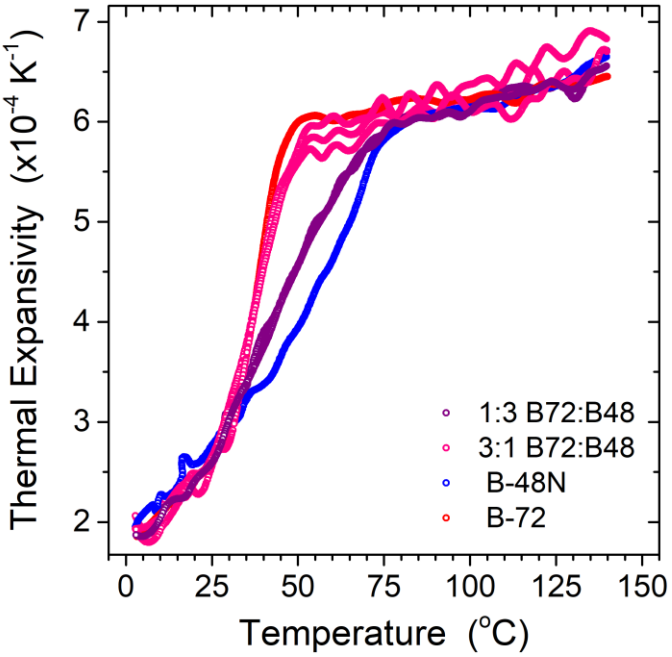

Figure 4.20: Thermal expansivity of B48N and B72 mixtures as a function of temperature, smoothed using the LOWESS method. The pink data are from samples consisting of a film of 3:1 mixture of B-72 and B-48N. The purple data are from samples consisting of a film of 1:3 mixture of B-72 and B-48. In order to be able to compare to the pure polymers, also shown are representative data of B-72 (red) and B-48N (blue).

The index of refraction of the films consisting of B-72 and B-48N in the 3:1 mixture, shown in Figure 4.18, present some slight variation that is caused by differences in the initial

alignment conditions of the ellipsometer. I measured an index of refraction at 30 °C of 1.471 ± 0.004 with an *A* value of 1.1.458 ± 0.005 and a *B* values of 0.0044 ± 0.0001 μm^2. The refractive index of the films consisting of a 1:3 B-72:B-48N mixture of those polymers has an index of refraction equal to 1.48 ± 0.001 at 30 °C, with an *A* value of 1.466 ± 0.001 at 30 °C and a *B* value of 0.00441 ± 0.00001 μm^2.

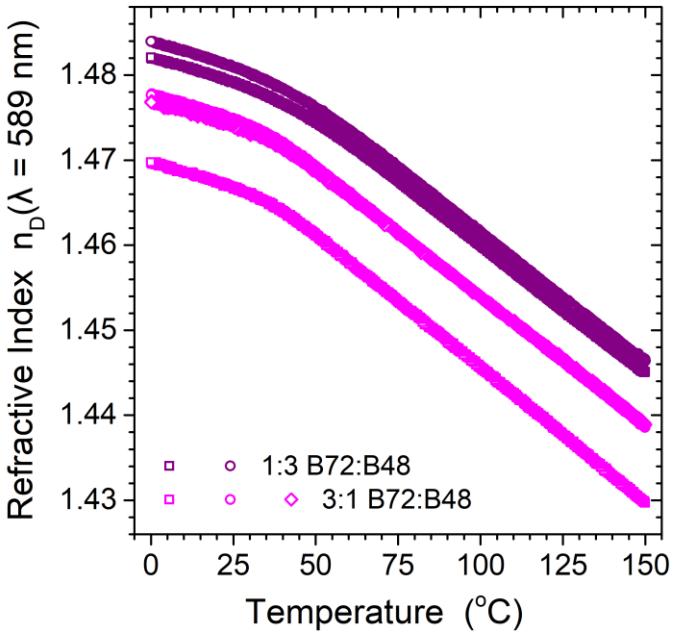

Figure 4.21: Refractive index of B-48N and B-72 mixtures as a function of temperature. The pink data are from samples consisting of a film of 3:1 mixture of B-72 and B-48N with thickness *h* = 1042 nm (circles), 996 nm (squares), and 1023 nm (diamonds). The purple data are from samples consisting of a film of 1:3 B-72:B-48N mixture of B-72 and B-48N with a thickness *h* = 859 nm (squares) and *h* = 851 nm (circles).

The data support the hypothesis that having a mixture of the two polymers will lead to better working properties because the higher blend T_g will lead to less issues of slumping or softening over time, while the smaller breadth of the transition will allow the polymer to be more uniform and easily annealed when used as an adhesive.[5,6,10]

4.7: Summary

In this chapter, I examined the properties of four polymers. The A-11 has, by far, the highest glass transition temperature, T_g, at 98 ± 2 °C, which explains its brittleness when used in art conservation, as the lack of annealing leaves solvent trapped inside the polymer even after it has become glassy. B-72, which is regarded as a polymer suited for almost every aspect of conservation,[10] has a glass transition of 40 ± 2 °C, which is comfortably above the temperature in museums. However, the glass transition is still occurring down to 25 °C which explains why the polymer can relax and allow all solvent to evaporate. The B-48N glass transition happens over a very broad temperature range and is still happening down to 0 °C, giving an artificially high calculated T_g of 55.6 ± 0.5 °C, while B-44 has a transition of 56 ± 2 °C, which is significantly higher than ambient temperature, explaining why it is often used as coating on outdoor sculptures.[10] Finally the mixtures of B-72 and B-48N were able to benefit from B-48's higher T_g, while still taking advantage of the short breadth of B-72's transition. These properties, as well as the other properties measured, are summarized in Table 4.1. The two samples of 1:3 B-72:B-48N polymer mixtures coincidentally happened to be very similar, and their value of B at 30 °C was identical, which is why the error for the sample is 0. The true sample error is likely comparable to those others measured.

Polymer	Sample thickness h(30 °C) (nm)	Average T_g (°C)	A(30 °C)	B(30 °C)	Refractive Index n(30 °C)
A-11	880 ± 40	98 ± 2	1.46 ± 0.05	4.41 ± 0.05	1.479 ± 0.003
B-72	940 ± 70	40 ± 2	1.461 ± 0.002	4.3 ± 0.5	1.474 ± 0.02
B-48N	910 ± 30	55.6 ± 0.5	1.4658 ± 0.00081	4.49 ± 0.04	1.4787 ± 0.0009
B-44	915 ± 5	56 ± 2	1.463 ± 0.003	4.8 ± 0.1	1.477 ± 0.003
1:3 B72:B48N	855 ± 5	47.3 ± 0.2	1.4666 ± 0.001	4.41 ± 0	1.479 ± 0.001
3:1 B72:B48N	1020 ± 20	44 ± 2	1.458 ± 0.004	4.4 ± 0.1	1.471 ± 0.004

Table 4.1: Summary of measured properties of samples discussed in this study.

Chapter 5: Conclusions

Art conservation regularly sees a need to repair or coat objects in non-climate controlled settings, but many of the commonly used polymers work best in the climate controlled setting of a museum, which is the setting for which they have been most studied. I used ellipsometry to measure the glass transition temperature, showing that ellipsometry is able to give values of T_g which match the literature. I also measured the refractive index as a function of temperature, showing that this too matched the literature data. Having confirmed that ellipsometry is able to measure accurate information of the samples, I was able to then study how polymer samples which were annealed to equilibrium went through the glass transition. Examining their thermal expansivity as a function of temperature revealed that some of the polymers' transition, notably that of B-48N was very broad. Despite having a T_g above 50 °C, B-48N does not reach a glassy state even at 0 °C.

Recently conservators have started using 3:1 mixtures of B72 and B-48N as it was observed to have better working properties,[5,6] mainly that it avoided B-72's tendency to creep when a force was applied over long periods of time. By studying the transition, I determined that this is because the addition of B-48N increased the T_g of B-72 while the B-72 prevented the large breadth of transition that happens in B-48N. The specific ratio had little effect, though, as would be expected, an increased amount of B-48N increased the T_g further at the expense of broadening the transition slightly. Mixtures of B-44 and B-72 may give the same higher T_g and outdoor stability as the mixtures of B-72 and B-48 and are worth studying in the future.

Now that ellipsometry has been established as a technique which allows us to measure information about the polymers that may be correlated to their working properties in art conservation, future work will study polymers which underwent non-ideal annealing procedures,

as happens in art conservation, as well as the effect of polymer composites which are often used in museums.

Chapter 6: References

(1) Horie, V. *Materials for Conservation: Organic Consolidants and Coatings*, 2nd ed.; Elsevier, 2010.

(2) Feller, R. L. *Accelerated Aging Photochemical and Thermal Aspects*; Getty Conservation Institute: Marina del Rey, CA, 1994; Vol. 44. https://doi.org/10.1016/j.lpm.2014.05.012.

(3) Koob, S. P. The Use of Paraloid B-72 as an Adhesive : Its Application for Archaeological Ceramics and Other Materials. *Stud. Conserv.* **1986**, *31* (1), 7–14.

(4) Andrew, O. *Reversibility: Does It Exist*; Oddy, A., Carroll, S., Eds.; The British Museum: London, 1999.

(5) Strahan, D.; Korolnik, S. Archaelogical Conservation. In *Troia 1987-2012: Grabungen und Forschungen I. Forschungsgeschichte, Methoden, und Landschaft.*; 2014; Vol. 1, pp 520–535.

(6) Riccardelli, C.; Morris, M.; Wheeler, G.; Soultanian, J.; Becker, L.; Street, R. The Treatment of Tullio Lombardo's *Adam* : A New Approach to the Conservation of Monumental Marble Sculpture. *Metrop. Museum J.* **2014**, *49* (1), 48–116. https://doi.org/10.1086/680027.

(7) Chiantore, O.; Lazzari, M. Photo-Oxidative Stability of Paraloid Acrylic Protective Polymers. *Polymer (Guildf).* **2001**, *42* (1), 17–27. https://doi.org/10.1016/S0032-3861(00)00327-X.

(8) Hiemenz, P. C.; Lodge, T. P. *Polymer Chemistry*, 2nd ed.; Taylor and Francis Group: Boca Raton, 2007. https://doi.org/10.1016/B978-1-84569-741-9.50002-1.

(9) Kawana, S.; Jones, R. A. L. Character of the Glass Transition in Thin Supported Polymer Films. *Phys. Rev. E - Stat. Physics, Plasmas, Fluids, Relat. Interdiscip. Top.* **2001**, *63* (2), 021501. https://doi.org/10.1103/PhysRevE.63.021501.

(10) Betz, J.; Wheeler, A. G. The Influence of Glass Transition Temperatures on the Performance of Acrylic Thermoplastic Adhesives, Columbia University Graduate School of Architecture, Planning, and Preservation, 2017.

(11) Derrick, M. Paraloid A-11. *Conservation and Art Materials Encyclopedia Online*; Museum of Fine Arts, Boston, 2018.

(12) Wunderlich, W. Physical Constants of Poly(Methyl Methacrylate). In *Polymer Handbook*; Brandrup, J., Immergut, E. H., Grulke, E. A., Abe, A., Bloch, D. R., Eds.; John Wiley & Sons, 2005; pp 87–90.

(13) Derrick, M.; Stacy, K.; Unckel, B. Paraloid B-72. *Conservation and Art Materials Encyclopedia Online*; Museum of Fine Arts, Boston, 2018.

(14) Derrick, M.; Ruggiero, J. Paraloid B-48N. *Conservation and Art Materials Encyclopedia Online*; Museum of Fine Arts, Boston, 2018.

(15) Derrick, M. Paraloid B-44. *Conservation and Art Materials Encyclopedia Online*;

Museum of Fine Arts, Boston, 2018.

(16) Chiantore, O.; Lazzari, M. Characterization of Acrylic Resins. *Int. J. Polym. Anal. Charact.* **1996**, *2* (4), 395–408. https://doi.org/10.1080/10236669608033358.

(17) Tompkins, H. G. *A User's Guide to Ellipsometry*; Academic Press: San Diego, Ca, 1993. https://doi.org/10.1002/9781119199090.fmatter.

(18) Huang, X.; Roth, C. B. Changes in the Temperature-Dependent Specific Volume of Supported Polystyrene Films with Film Thickness. *J. Chem. Phys.* **2016**, *144* (23), 234903. https://doi.org/10.1063/1.4953855.

(19) OriginLab Corporation. 18.1.2 Algorithms (Smooth) https://www.originlab.com/doc/Origin-Help/Smooth-Algorithm.